Published in final edited form as:
J Comp Neurol. 2010 April 1; 518(7): 1046–1063. doi:10.1002/cne.22262.

Synaptic Plasticity after Chemical Deafening and Electrical Stimulation of the Auditory Nerve in Cats

D.K. Ryugo[1,2], **C.A. Baker**[1], **K.L. Montey**[1,3], **L.Y. Chang**[1], **A. Coco**[4], **J.B. Fallon**[4,5], and **R.K. Shepherd**[4,5]

[1] Department of Otolaryngology-HNS, Johns Hopkins University School of Medicine, Baltimore, MD 21205, USA

[2] Department of Neuroscience, Johns Hopkins University School of Medicine, Baltimore, MD 21205, USA

[3] Department of Biology, University of Maryland, College Park, MD 20742, USA

[4] The Bionic Ear Institute, Melbourne, Victoria 3002, Australia

[5] Department of Otolaryngology, University of Melbourne, Victoria 3002, Australia

Abstract

The effects of deafness on brain structure and function have been studied using animal models of congenital deafness that include surgical ablation of the organ of Corti, acoustic trauma, ototoxic drugs, and hereditary deafness. This report describes the morphologic plasticity of auditory nerve synapses in response to ototoxic deafening and chronic electrical stimulation of the auditory nerve. Normal kittens were deafened by neonatal administration of neomycin that eliminated auditory receptor cells. Some of these cats were raised deaf, whereas others were chronically implanted with cochlear electrodes at two months of age and electrically stimulated for up to 12 months. The large endings of the auditory nerve, endbulbs of Held, were studied because they hold a key position in the timing pathway for sound localization, are readily identifiable, and exhibit deafness-associated abnormalities. Compared to normal hearing cats, synapses of ototoxically deafened cats displayed expanded postsynaptic densities, a decrease in synaptic vesicle (SV) density, and a reduction in the somatic size of spherical bushy cells (SBCs). When compared to normal hearing cats, endbulbs of ototoxically deafened cats that received cochlear stimulation expressed postsynaptic densities (PSDs) that were statistically identical in size, showed a 32.8% reduction in SV density, and whose target SBCs had a 25.5% reduction in soma area. These results demonstrate that electrical stimulation via a cochlear implant in chemically-deafened cats preserves PSD size but not other aspects of synapse morphology. The results further suggest that the effects of ototoxic deafness are not identical to those of hereditary deafness.

Keywords

cochlear implant; deafness; electrical stimulation; endbulb of Held; ototoxicity

It is well known that sound stimulation has an important role in the structural and functional development of the central auditory system. The importance of auditory stimulation is especially manifest in the developing animal as deprivation early in the postnatal period produces severe abnormalities in the auditory pathways; in mature animals with previous

Corresponding author: Center for Hearing and Balance, Johns Hopkins University School of Medicine, 720 Rutland Ave., Baltimore, MD 21205, Phone 410-955-4543, Fax 410-955-1317, dryugo@jhu.edu.

auditory experience these effects are diminished (Powell and Erulkar, 1962; Webster, 1983a,b; Rubel and Parks, 1988; Shepherd et al., 2006). These observations have been associated with the age-related benefits of cochlear implantation in congenitally deaf humans (Quittner and Steck, 1991; Waltzman et al., 1991; Gantz et al., 1994) because younger children typically gain more benefit from a cochlear implant than older children. These data imply that deafness causes change in the central nervous system that, if not corrected, interferes with implant effectiveness.

Cochlear implants bypass the nonfunctioning hair cell receptors of the inner ear by directly stimulating the auditory nerve. The auditory nerve delivers this information to the cochlear nucleus, which in turn distributes outgoing messages to higher centers. This circumstance makes the synaptic relationships between auditory nerve fibers and cochlear nucleus neurons key to central auditory processing. It is in this context that we have chosen to study endbulbs of Held, the large axosomatic endings of auditory nerve fibers which initiate a pathway to process binaural timing cues.

In the congenitally deaf white cat, pathologic changes initiated at the organ of Corti continued transsynaptically along the auditory pathways including synaptic abnormalities in auditory nerve endings (Ryugo et al., 1997, 1998) and somatic shrinkage at higher centers (West and Harrison, 1973; Schwartz and Higa, 1982). Moreover, there was physiological evidence for pathology in the intrinsic microcircuitry of auditory cortex (Kral et al., 2006). Our working hypothesis was that the failure of auditory nerve synapses to convey spike activity to the central auditory pathways mediated these central effects. A corollary to this idea is that a reintroduction of activity in the auditory nerve by surgically placing unilateral cochlear implants into congenitally deaf cats would repair the system (Kretzmer et al., 2004). In fact, electrical stimulation of the cochlea in deaf white cats was shown to restore the morphology of auditory nerve synapses in the cochlear nucleus (Ryugo et al., 2005) and to recruit neural responses in auditory cortex that more resembled those in normal hearing cats (Klinke et al., 1999).

The striking corrective effects of electrical stimulation on deaf white cats prompted us to ask if these plastic changes in the brains of genetically deaf cats represented common features that could be observed in other models of acquired congenital deafness. In one well-established model, deafness is produced by the administration of ototoxic drugs to newborn normal hearing kittens. These drugs include aminoglycoside antibiotics (e.g., amikacin, neomycin, and kanamycin), salicylates, anti-neoplastics (cisplatin), and diuretics (ethacrynic acid and furosemide) and are known to cause loss of hair cell receptors during onset of normal hearing (Hawkins, 1973; Leake and Hradek, 1988; Lustig et al., 1994; Shepherd and Hardie, 2001). Since the mechanisms underlying ototoxic deafness and hereditary deafness are undoubtedly different, we sought to determine how synapses of auditory nerve fibers responded to ototoxic deafness and to the restoration of its activity by electrical stimulation of the cochlea.

Materials and Methods

Subjects

Normal hearing cats were purchased from a licensed vendor (The Biological Research Centre, Department of Otolaryngology, University of Melbourne, Melbourne, Australia) and bred in the lab. Cats from individual litters were raised together but assigned to one of three cohorts: normal controls, deafened, and deafened and electrically stimulated. Animals were weaned at 8 weeks. All procedures were approved by and conducted under the auspices of the Animal Research Ethics Committee, Royal Victorian Eye and Ear Hospital, Melbourne, Australia.

Deafening procedure

Neomycin (60mg/kg SC, Sigma) was administered daily (for a minimum of 17 days) beginning on postnatal day 1 (Leake et al., 1999). Hearing status was assessed by recording click-evoked Auditory Brainstem Responses (ABRs) at postnatal day 17. Cats with no evidence of an ABR to a 98 dB peak equivalent SPL click were considered profoundly deaf and received no further neomycin administration. Neomycin administration was continued in animals with a recordable ABR and their hearing tested every three to four days until they had no response. The duration of the neomycin administration for each animal is listed in Table 1, and there was no difference in duration of the deafening protocol for the deaf vs deaf/stimulated groups (Mann-Whitney Rank Sum Test; $P > 0.09$).

Auditory Brainstem Responses

ABRs were recorded in an electrically isolated, sound-attenuated Faraday room. The animals were premedicated with Xylazine (2 mg/kg, SC), and then sedated with Ketamine (20 mg/kg, IM). During recording, the animal's temperature was maintained at 37±1°C. Computer generated 100 μs rarefaction clicks were presented from a loudspeaker placed 10 cm from the pinna. The contralateral external ear canal was plugged with an ear mould compound (Otoplastik, Unna, Germany). ABRs were recorded differentially using subcutaneous stainless steel electrodes (vertex positive, neck negative, and thorax ground). The stimuli were presented at a rate of 33 per second. The responses were amplified by a factor of 10^5, and filtered through a band-pass filter (high pass: 150 Hz, 24 dB/octave; low pass: 3 kHz, 6 dB/octave). The output of the amplifier was fed to a 10-bit AD converter and sampled at 20 kHz for a period of 12.5 ms following stimulus onset. Five hundred responses were averaged and stored for subsequent automated computer analysis, performed with Igor Pro (WaveMetrics, Portland, OR) using custom-written analysis procedures. Two recordings were made at each stimulus level. An attenuator was used to reduce the intensity of the acoustic stimulus to determine threshold, which was defined as the minimum stimulus required to produce a wave IV (approximately 4.0–4.5 ms latency relative to the stimulus onset) amplitude of at least 0.2 μV in 2 repeated recordings.

Electrical ABRs

Electrically-evoked auditory brainstem responses (EABRs) were recorded differentially as in the ABR procedure described above. Optically isolated biphasic current pulses (100 μsec per phase; 50 μsec interphase gap) were generated under computer control and delivered to a pair of electrodes on the intracochlear electrode array. Responses were recorded using the same techniques as described for the ABR except for the inclusion of a sample-and-hold circuit in order to remove electrical artifact (Black et al., 1983). Two recordings were made at each current level and current amplitude was reduced to levels below threshold. Threshold was defined as the smallest current level required to evoke a peak-trough response amplitude of at least 0.2 μV for wave IV of the EABR (within a latency window of 2.4–2.9 ms following stimulus onset) for both responses. These recording procedures were similar to those previously published (Coco et al., 2007).

Stimulation Methods

Each animal that was to receive chronic electrical stimulation was unilaterally implanted at eight weeks of age with an intracochlear electrode array and lead-wire assembly using previously published techniques (Coco et al., 2007). The electrode arrays contained eight platinum electrodes with surface areas of approximately 0.42 mm2 and were inserted approximately 8 mm into the scala tympani via a small incision in the round window. This insertion depth placed the most apical electrode at the ~10 kHz position in the cochlea and the most basal electrode at the 26 kHz position (Brown et al., 1992). Fourteen days following

implant surgery a chronic electrical stimulation program commenced using Nucleus® CI24 cochlear implants in combination with Nucleus® ESPrit 3G behind-the-ear speech processors (Cochlear Ltd). Implantation and stimulation turn-on was delayed until this age to allow the animals to fully recover from the deafening procedure, and stimulation from this age has been shown to be early enough to produce significant functional change (e.g. Fallon et al., 2009).

The implant electrodes were connected to a percutaneous lead-wire system and carried in a harness worn by the animals to enable continuous stimulation without confining their daily activities. Each animal's processor was programmed to deliver stimulation at levels between 3dB below the EABR threshold and 6dB above the EABR threshold (i.e., T-level= 3dB below EABR threshold and C-level= 6dB above EABR threshold). These levels were confirmed to be well tolerated by the animals and all animals exhibited behavioral responses (orienting responses including head and pinna movements) to their acoustic environment, which included sounds associated with the normal running of such a facility. Additionally, it was confirmed that both self-vocalizations and vocalizations by other animals housed in the facility produced changes in the stimulus levels that were within the perceivable range for each animal. The output of the stimulator delivered 100 μs/phase charge-balanced biphasic current pulses to electrodes in either bipolar or common ground configuration (see Table 1), at a stimulus rate of 500 pulses per second per electrode. The maximum stimulus current amplitudes used in this study were in the range 200–500 μA at 100 μs/phase, which produced charge densities of 4.8 – 11.9 $\mu C/cm^2$. Stimulated animals received stimulation 24 hours/day, 7 days per week and their battery supply was checked and maintained daily.

Histologic Procedures

Animals were administered a lethal dose of sodium pentobarbital (65 mg/kg, IV) and when areflexic to corneal stimulation, were perfused through the heart with 25 cc of 0.1 M phosphate buffered isotonic saline with 0.5% $NaNO_2$ (pH 7.4) followed immediately by 2 L of a 0.1 M phosphate buffered solution containing 2% paraformaldehyde and 2% glutaraldehyde. Following perfusion, subjects were decapitated and the head immersed in the same fixative (5° C) with just enough bone removed to expose the brain stem and cochlear nuclei to fixative. The cochleae were harvested (see below). The next day, the brains were dissected from the skull, and the cochlear nuclei dissected and embedded in a gelatin-albumin mixture hardened with glutaraldehyde. The tissue block was sectioned in the coronal plane (50–75 μm thickness) on a Vibratome. Sections were collected in serial order and separated into two series: one for light microscopy and one for electron microscopy. Those sections for electron microscopic analysis were placed in 1% OsO_4 for 15 minutes, rinsed in buffer, bloc stained in 1% uranyl acetate, rinsed, dehydrated in an ascending concentration of alcohols, and flat embedded in PolyBed 812 between two sheets of Aclar. After polymerization, pieces of the rostral anteroventral cochlear nucleus (AVCN) were cut out and re-embedded in BEEM capsules. Ultrathin sections were collected from the appropriate frequency region of the AVCN (dorsal to the 10 kHz isofrequency contour, Bourk et al., 1981) that was consistent with the frequency region stimulated by the implant, placed on Formvar-coated slotted grids, and examined in an electron microscope.

Cochlear preparation

Immediately following the transcardial perfusion, the cochleae were dissected from the skull and the oval and round window membranes were incised under microscopic observation. The cochleae were then placed in the same fixative solution overnight. The cochleae were decalcified (10% EDTA in 10% neutral buffered formalin), dehydrated, embedded in Spurr's resin and serially sectioned at a thickness of 2 μm through the midmodiolar region and stained with hematoxylin and eosin (H&E).

Data analysis

Spiral ganglion neuron (SGN) density was measured by a single observer, blind to the experimental group. For each midmodiolar section (n=6 per cat), the basal cochlear turn was identified and the cross sectional area of Rosenthal's canal was measured using NIH image (http://rsb.info.nih.gov/nih-image/). Neurons within Rosenthal's canal with a clearly visible nucleolus were counted (40x objective, NA 0.70) and SGN density calculated as cells/mm^2. As a single nucleolus was never visible in two adjacent sections (i.e., it can be considered a point source), this counting technique provides an estimate that needs no corrections (Guillery, 2002).

Endbulbs of Held make contact with spherical bushy cells and are distributed in the rostral pole of the AVCN. Endbulb identification was based on previously published criteria showing their distinct properties at the ultrastructural level (Lenn and Reese, 1966; Gentschev and Sotelo, 1973; Cant and Morest, 1979; Ryugo et al., 1996, 1997). All tissue was coded so that observers were blinded to the treatment group. Unbroken strings of 20–30 serial sections were collected from endbulbs of normal hearing cats (n=3 cats, 20 endbulbs), deafened cats (n=3 cats, 27 endbulbs) and deafened and stimulated cats (n=5 cats, 34 endbulbs). Endbulbs were randomly selected from each animal for electron microscopic analysis. Each photomicrograph was digitized, and the perimeter of each endbulb profile and length of every postsynaptic density (PSD) were traced; these outlines were aligned and stacked using *Adobe Photoshop 7* and imported to *Amira 4.0* (Mercury Systems, Carlsbad, CA). Three-dimensional reconstructions of each endbulb were made and the surface area measured; the area measurements incorporate the curvature of the PSD.

The number of synaptic vesicles (SVs) in a 0.5-μm radius of the PSD was counted from randomly selected endbulbs of each animal by a "blinded" observer. Counts were "corrected" according to a modification of Abercrombie's (1946) formulation. Because synaptic vesicles are ring-shaped, we only counted structures that exhibited a complete ring with a clear lumen, and were <80 nm in diameter. Those SVs whose luminal-points were outside the ultrathin section but which were nevertheless represented by fragments inside the section, have their luminal-points extending through a volume of tissue equivalent to, on average, of the inside diameter of the SV. SV fragments without a lumen were effectively ignored which is why the diameter of the SV was not used. Instead we measured the maximum luminal diameter (from the inner edge of the SV membrane on one side to the inner edge of the SV membrane on the opposite side) for a minimum of 100 SVs (range 112–311). The mean luminal diameter, *M*, was used in the formula $P=A(T/T+M)$ to calculate the corrected count *P* where *A* equals the uncorrected count and *T* equals the ultrathin section thickness. Maximum SV diameters was measured by placing the "crosshair" of the ruler in Photoshop over the opposing outside edges of the SV membrane in *Photoshop*.

To determine this area within the endbulb, the center of a 1-μm diameter pencil in *Adobe Photoshop* (Ryugo et al., 2006) was run along the PSD; mitochondria and inclusions were subtracted to yield cytoplasmic area. SV density was calculated by dividing the corrected vesicle count by the area of the 0.5-μm PSD radius within the endbulb. By restricting the vesicle counts to the area immediately surrounding the PSD, regions of axoplasm (which lack vesicles) were eliminated and counts focused on vesicles that appeared most ready for release. If PSDs were within 0.5 μm of each other, they were considered a single structure for the purpose of determining vesicle density so that no vesicle was counted twice. Digital images of endbulb profiles were collected at 15,000x at 328 pixels/inch and analyzed at 100% magnification. A three-pixel dot was placed in the lumen of every SV in the defined radius. Area measurements and SV counts were made with *ImageJ v1.32* (NIH) and were expressed as mean ± 1 standard deviation.

Results

The present results are based on data collected from three normal hearing cats, three ototoxically deafened cats, and five ototoxically deafened cats that were implanted at 8 weeks of age with chronic scala tympani electrode arrays (Table 1). The hearing status of each cat was evaluated periodically during the course of the experiment. Hearing cats exhibited ABRs in response to 20 dB peak equivalent SPL clicks, whereas deafened cats exhibited no response to clicks up to 98 dB peak equivalent SPL, consistent with previous results from the lab using aminoglycoside-based deafening procedures (e.g., Coco et al., 2007).

The histological appearance of the organ of Corti and spiral ganglia was consistent with each cat's hearing status (determined by the presence or absence of sound-evoked activity). Hearing cats exhibited a normal organ of Corti and spiral ganglia. Inner and outer hair cells, Reissner's membrane, the tectorial membrane, and type I and type II ganglion cells were evident all along the cochlear duct, from the apex to base (Fig. 1A, A′). In contrast, the chemically-deafened cats had no hair cells present and the organ of Corti was completely absent in the basal turn (Fig. 1B). There was also widespread spiral ganglion neuron loss that was greater in the basal and middle turns compared to the apical turn (Fig. 1B′). Deafened cats that received unilateral electrical stimulation also exhibited complete loss of hair cells throughout the cochlea and a loss of the organ of Corti in the basal turn (Fig. 1C). Substantial ganglion neuron loss was evident (Fig. 1C′), and as in the nonstimulated deafened cochleae, the loss was variable along Rosenthal's canal with greater loss occurring in the base. Histological analysis demonstrated that there were no acoustic receptors in the deafened cats but there were residual ganglion cells giving rise to fibers of the auditory nerve.

Spiral Ganglion Cells

The density of spiral ganglion cells (SGCs) was calculated for the region of Rosenthal's canal that lay alongside of the cochlear implant electrode array. The mean ganglion cell density in normal hearing cats is 889.6 ± 240 cells/mm^2. In contrast, the mean cell density for deafened cats was 177 ± 101 cells/mm^2 and for electrically stimulated deafened cats 205.7 ± 123.8 cells/mm^2. There was no statistical difference between the latter two cohorts but the normal hearing cats had statistically greater density values ($p<0.001$, Kruskal-Wallis test).

Auditory Nerve Endings

In the AVCN, endbulbs of the auditory nerve present ultrastructural characteristics that make them clearly identifiable, even under pathologic conditions. Endbulbs are large, but in ultrathin sections, tangential views often present only small portions of the structure. Nevertheless, the cytoplasm is lighter in density than other endings, and there is a distinct covering of glial lamellae. Auditory nerve endings contain clear, round SVs (approximately 45–50 nm in diameter) and exhibit paired but asymmetric membrane thickenings with the somata of spherical bushy cells (Fig. 2A–D, asterisks). In normal hearing cats, the presynaptic membrane thickening is thinner than the postsynaptic membrane thickening, and marked by an associated cluster of synaptic vesicles. The asymmetric membrane thickenings are dome-shaped, arch into the presynaptic endbulb, and represent the synaptic release sites. We focused on the postsynaptic thickening or density (PSD) because it was so much more prominent than the presynaptic thickening. When individual synapses were followed through consecutive serial sections, PSDs were reconstructed in three dimensions using computer software and rotated 90 for an *en face* view. In this way, individual PSDs could be seen lying on the surface of the postsynaptic membrane and their discrete nature revealed (Fig. 2E). The reconstructed, three-dimensional surface area of individual postsynaptic densities (n=107) from 20 endbulbs of normal hearing cats averaged 0.100 ± 0.06 μm^2.

The endbulbs of ototoxically deafened cats exhibited distinct structural differences when viewed in an electron microscope (Fig. 3A–F). The auditory nerve endings tended to partially embed themselves in the postsynaptic cell body (white arrows in Fig. 3B, C, F). Normally, these endings reside on the surface of the SBC (Fig. 3D). There was a reduction in the number of clear round SVs and the PSDs appeared flatter, thicker, and longer. That is, the punctate arched appearance of the PSDs was replaced by a broader curve (Fig. 3D, E) or a wavy shape (Fig. 3A, B, C, F). Individual PSDs (n=184) were reconstructed through serial sections from 27 endbulbs and observed to be hypertrophied (Fig. 3G). These PSDs averaged 0.164 ± 0.20 μm^2.

In deafened cats that were stimulated electrically via a cochlear implant, endbulb synapses ipsilateral to the cochlear implant resembled those of normal hearing cats except SV density did not increase to normal levels (Fig. 4A–D). A small proportion of endings appeared sunken into the cell body but the punctate and distinctive dome-shape of the normal PSDs returned. Glial lamellae were present around these primary endings. The PSDs (n=167) from 34 endbulbs of five implanted cats were reconstructed through serial sections; they were essentially normal in size (0.127 ± 0.10 μm^2) and spatial distribution (Fig. 4E). A view of the reconstructed PSDs is summarized (Fig. 5). Nonparametric analysis (Kruskal-Wallis test) revealed that on average, there was no significant difference between the size of PSDs from the auditory nerve fibers of normal hearing and deaf-stimulated cats, whereas those from unstimulated deafened cats were significantly larger ($p < 0.05$). A plot of all PSD values is provided (Fig. 6). Moreover, PSD size was not correlated with duration of electrical stimulation or age of animal ($p>0.1$, Pearson product-moment coefficient).

Analysis of SV density revealed a statistically significant difference in SV density between hearing cats and deaf cats with or without electrical stimulation ($p < 0.001$, Kruskal-Wallis Test) and there was no difference in SV density between congenitally deaf cats and deaf cats with cochlear implants. The concentration of SVs within 0.5 μm of the PSD for normal hearing cats was 74.40 ± 16.6 SV/μm^2; the value for ototoxically deafened cats was 48.07 ± 24.8 SV/μm^2; and the deafened/stimulated cats had the lowest SV density at 38.63 ± 18.3 SV/μm^2. The maximum diameter of SVs for all cats was 45.3–48.3 nm, and there was no statistical difference among individual cats or across cohorts ($p>0.05$, Tukey-Kramer HSD). These results are illustrated by representative electron micrographs (Fig. 7).

Spherical Bushy Cells

We measured the cell body area of SBCs of the cochlear nucleus. Because cell bodies are known to shrink as a result of deafness (West and Harrison, 1973; Larsen and Kirchoff, 1992; Saada et al., 1996), the hypertrophied PSDs could simply reflect their merging due to a smaller surface area. Spherical bushy cells in the 10 kHz and higher frequency region (Bourk et al., 1981) of the anterior division of the AVCN were selected to ensure that we were sampling from cells that would most likely be stimulated by the indwelling basal cochlear electrodes. A minimum of 100 cells per cochlear nucleus was drawn using 100x oil immersion lens (total magnification of 1250x) and a drawing tube attached to a light microscope. Somatic silhouette areas were calculated using NIH *Image J* software (Fig. 8). Spherical bushy cells from normal hearing cats had a mean somatic area of 586.14 ± 87.8 μm^2. Those from ototoxically deaf cats averaged 494.91 ± 65.2 μm^2, exhibiting a 15.6% reduction. Electrical stimulation of the auditory nerve did not have a restorative effect on cell body size for ototoxically deaf cats (mean cell body size = 372.9 ± 72.9 μm^2). Cell body size of normal hearing cats was significantly larger than those of unstimulated deaf cats (ANOVA, $p <0.05$), and unstimulated deaf cats had cell body sizes that were on average statistically larger than those of deaf cats that received electrical stimulation ($p<0.05$). There was no statistical difference in somatic size

when comparing the ipsilateral stimulated side to the contralateral side (390.8 ± 62.9 μm^2, $p > 0.85$).

Discussion

The present results add to on-going studies of plasticity in the central auditory system in response to deafness and electrical stimulation via a cochlear implant (e.g., Ryugo et al., 2005; Fallon et al., 2009). These studies explore the replacement effects of afferent input to a deaf auditory system. Our results show that chronic intracochlear electrical stimulation restores the size of auditory PSDs but does not rescue SV numbers, SGC density, or SBC somatic size (Fig. 9). It should be noted that normal hearing cats, whether raised in the USA or Australia, exhibit smaller PSDs compared to those of hereditary and ototoxically deafened cats (Ryugo et al., 2005). A direct comparison is not possible, however, because the earlier study calculated PSD size from two-dimensional flattened images (*ImageJ*), whereas the current study calculated PSD size in three-dimensions (*Amira*). The observation that electrical stimulation remediates some but not all features of the relationship between auditory nerve fibers and SBCs is consistent with the idea that the two models for congenital deafness, hereditary deaf white cats and ototoxically deafened normal cats, are qualitatively similar.

We further demonstrate that electrical stimulation in the deafened cochlea does not provide trophic support of SGCs, since the SGC density of electrically stimulated cochleae exhibited no evidence of increased survival compared with the deafened, unstimulated controls. These results are consistent with previous data from our laboratory (Coco et al., 2007; Shepherd et al., 2005; Shepherd et al., 1994), but differ with the findings of other groups that have reported a modest but significant trophic influence on SGCs following chronic electrical stimulation (Hartshorn et al., 1991; Leake et al., 1991, 1999; Mitchell et al., 1997).

Under normal conditions, auditory nerve fibers exhibit spontaneous spike discharges, ranging from near zero to more than 100 spikes/sec (Kiang et al., 1965; Liberman, 1978). Those fibers exhibiting lower levels of spontaneous and evoked activity have larger and flatter PSDs; in contrast, those with higher levels of activity exhibit smaller and distinctly curved PSDs (Ryugo et al., 1996). Heredity congenital deafness in white cats eliminates most activity in auditory nerve fibers (Ryugo et al., 1998) with a resulting flattening and hypertrophy of PSDs in their large endings (Ryugo et al., 1997). The relationship between congenital deafness and abnormal synapse structure was replicated in the *Shaker-2* mouse (Lee et al., 2003). In deaf white cats, the restoration of spike activity in the auditory nerve using a cochlear implant preserved normal synapse morphology in the ipsilateral endbulbs of Held (Ryugo et al., 2005). Ototoxic deafness resembles hereditary deafness by causing organ of Corti destruction during development and significantly reducing the level of spontaneous and driven activity in the auditory nerve (Shepherd and Javel, 1997).

One question is whether the hypertrophy of PSDs was merely a simple consequence of surface area shrinkage of the spherical bushy cell, as it is well known that deafness causes somatic shrinkage of cells in the cochlear nucleus (Powell and Erulkar, 1962; West and Harrison, 1973; Trune, 1982; Moore and Kowalchuk, 1988; Hultcrantz et al., 1991; Moore et al., 1994; Saada et al., 1996). With shrinkage, there would be a corresponding loss of somatic surface area, and it follows that individual PSDs might simply coalesce into larger units. With replacement of auditory nerve activity via electrical stimulation of the cochlea, it has also been reported that spherical cell body size increases (Lustig et al., 1994). The resulting expansion of surface area would presumably allow PSDs to resume their normal size and shape. Our results, however, revealed that electrical stimulation of the cochlea had an effect on PSD size that is independent of spherical bushy cell size and spiral ganglion cell density (Fig. 9). These

data suggest that morphological plasticity of the PSDs in spherical bushy cells is not a passive reflection of available somatic surface area.

The restoration of PSD size following electrical stimulation in ototoxically deafened cats resembles that observed in hereditary deafness (Ryugo et al., 2005; O'Neil et al., 2009). The magnitude of the restoration was smaller than that from hereditary deafness because the hypertrophy of the PSDs was reduced. One possibility for this more moderate reaction is that these animals experience some auditory experience. During the time required to deafen the developing animals by the ototoxic drugs (a minimum of 17 days), some amount of hair cell stimulation could have occurred because hair cell sensitivity to ototoxic drugs is inversely related to age (Shepherd and Martin, 1995). Early hearing experience could be sufficient to mute the PSD hypertrophy.

The smaller hypertrophy of PSDs in this study could also indicate that ganglion cells are undergoing some degenerative change. There is a more extensive and faster loss of spiral ganglion cells with ototoxic deafness compared to that in hereditary deafness (Mair, 1973; Webster and Webster, 1981; Keithley and Feldman, 1983; Hardie and Shepherd, 1999; Leake et al., 2008). In hereditary deafness, SV density increases by nearly 50% but returns to near normal values after electrical stimulation (O'Neil et al., 2009). This increase does not occur in ototoxic deafening. It is not unreasonable to expect the active process of up- and down-regulation of PSD proteins in the cochlear nucleus to be influenced by the relative health of the system.

When comparing data between ototoxically deafened cats and hereditary deafened cats, it is important to remember the general observation that the longer the period of deafness, the more severe the functional (Shepherd et al., 2004) and structural (Moore et al., 1994; Sly et al., 2007) changes. If one accepts that electrical stimulation via a cochlear implant "eliminates" deafness, then the ototoxically deafened cats have a shorter duration of deafness because they begin their stimulation program at 2 months of age. In contrast, the hereditary deafened cats begin their stimulation at 3 months of age (Ryugo et al., 2005). This circumstance implies that the deaf white cats might exhibit more severe abnormalities compared to the ototoxically deafened pigmented cats. Because such is not the case at the end of the stimulation period, the cause of differences in deafness-induced abnormalities between the two model systems remains undetermined.

Plasticity in synaptic structure due to deafness and stimulation

The synapses of endbulbs are normally small and discrete (Ryugo et al., 1996). It has been speculated that discrete PSDs improve glutamate diffusion kinetics. Circumscribed release sites with associated receptors would facilitate the near simultaneous binding of neurotransmitter and its rapid dispersion, thereby facilitating the rapid time course of excitatory postsynaptic currents (Matsuzaki et al., 2001; Franks et al., 2002). The morphology of endbulb synapses are optimally efficient when there is a high demand for spike activity, and their target SBCs are known for their ability to fire at high rates (Moller, 1969; Babalian et al., 2003).

The size of endbulb-associated PSDs is inversely correlated with levels of activity (Ryugo et al., 1996, 1998). In principle, synaptic strength would be affected by changes in postsynaptic receptor accumulation. Changes in excitatory synaptic transmission are accompanied by changes in AMPA receptor density (Lissin et al., 1998) and the postsynaptic sensitivity to glutamate (O'Brien et al., 1999; Turrigiano et al., 1998). Importantly, activity blockade significantly increased the postsynaptic accumulation of synaptic AMPA receptors (Wierenga et al., 2005). These observations imply a significant role for spike activity on the synaptic dynamics of auditory nerve fibers.

Functional significance of synaptic plasticity

The synaptic abnormalities of endbulbs resulting from untreated, early onset deafness (e.g., Ryugo et al., 1997, 1998) could represent one of the substrates that impairs transmission within the central auditory pathways when cochlear implants are used. Such would be the case if cochlear implantation, when performed in older children or adults, did not restore auditory nerve synapses to their natural state; the outcome would be minimal benefit in terms of speech perception (Waltzman et al., 1991; Niparko et al., 2000; Busby, 1993). Evidence for a critical period has been provided where electrical stimulation via cochlear implants in three-month old congenitally deaf cats resulted in the restoration of auditory nerve synapses, whereas that in six-month old congenitally deaf cats had no effect (O'Neil et al., 2009). The collective body of literature emphasizes the importance of the auditory nerve synapses for faithfully furnishing sound information to the central pathways. This initial stage of the system probably does not underlie sound cognition but certainly enables such higher order processing.

The loss of SVs and less efficient receptor system might reduce the ability for auditory synapses in congenitally deaf animals to transmit with high fidelity (Oleskevich and Walmsley, 2002). Synaptic failure at the spherical bushy cell would have a major impact on the "timing" pathway for terrestrial mammals, compromising neural processing at the level of the superior olivary complex and higher. If synaptic "jitter" were introduced at auditory stations along the ascending pathway, then there could be an overall reduction in the synchrony of the afferent volley. The consequence of this situation might be a reduction and latency increases in EABR peaks. Consistent with this idea, there were conspicuous deficits in the synaptic activity in the infragranular cortical layers of cat auditory cortex, implying that the thalamocortical volley was compromised (Kral et al., 2000).

EABRs elicited from deafened animals show marked decreases in amplitude and amplitude-level slope and increases in both threshold and latency compared to normal controls, with more marked changes evident with longer durations of deafness (Hardie and Shepherd, 1999); similar changes have also been reported clinically (Firszt et al., 2002; Thai-Van et al., 2002). Some of these functional changes may be associated with changes in response properties of spiral ganglion neurons in deafened animals (Shepherd and Javel, 1997), whereas others may be related to changes in more central auditory nuclei, such as a reduction in the number, strength or atrophy of excitatory synapses (Kotak and Sanes, 1997; Ryugo et al., 1997; Hardie et al., 1998).

The plastic changes in the ultrastructure of the endbulb may have pertinent clinical implications, particularly associated with the application of cochlear implants. For example, normal hearing subjects are sensitive to interaural time delays (ITDs) as narrow as 10–20 μsec (Yost, 1974). These ITD thresholds are typically an order of magnitude shorter than those of bilateral cochlear implant recipients (van Hoesel and Tyler, 2003; Laback et al., 2004), although balanced bilateral hearing is a positive factor in spatial hearing (e.g., direction, distance, movement) and is associated with an improvement in sound quality (Nobel and Gatehouse, 2004). If endbulb-spherical bushy cell synapses remain abnormal after chronic electrical stimulation, a reduction in resolution in spike timing at the level of the spherical bushy cell is likely to contribute to the reduced ITD sensitivity reported for bilaterally implanted subjects. The restoration of this synapse by electrical stimulation following congenital deafness (Ryugo et al., 2005) argues strongly for early implantation.

In summary, our results demonstrate that deafness, regardless of the cause, exerts profound effects on synaptic structure. Moreover, when spike activity is restored to the auditory nerve by electrical stimulation from a cochlear implant, there is a tendency toward the restoration of synaptic structure but the functional consequences of the preservation is yet to be determined.

These plastic phenomena in ototoxically deafened cats appear muted at the auditory nerve synapse compared to that observed in genetic deafness for the deaf white cat (Ryugo et al., 2005), but nevertheless establishes a generality of effects for these two models of congenital deafness.

Acknowledgments

This research was supported by NIH/NIDCD grants DC00232 and T32 DC00046, NIH/NIDCD contracts N01-DC-3-1005 and HHS-N-263-2007-00053-C, the Victorian State Government, the Royal Victorian Eye and Ear Hospital, the Emma Liepmann Endowment, Advanced Bionics Corporation, and Cochlear Corporation.

Special thanks are extended to Mr. Tan Pongstaphone for his technical assistance with electron microscopy, Ms. Lauren Donley for animal maintenance, Dr. Jin Xu and Ms. Helen Feng for electrode manufacture, Ms. Maria Clark for histology, Ms. Elisa Borg for animal husbandry, and Mr. Rodney Millard, Dr. Peter Seligman and Dr. John Heasman for expert engineering assistance and advice.

References

Abercrombie M. Estimation of nuclear population from microtome sections. J Anat 1946;94:239–247.

Babalian AL, Ryugo DK, Rouiller EM. Discharge properties of identified cochlear nucleus neurons and auditory nerve fibers in response to repetitive electrical stimulation of the auditory nerve. Exp Brain Res 2003;153:452–460. [PubMed: 12955378]

Black RC, Clark GM, O'Leary SJ, Walters C. Intracochlear electrical stimulation of normal and deaf cats investigated using brainstem response audiometry. Acta Oto-Laryngol Suppl 1983;399:5–17.

Bourk TR, Mielcarz JP, Norris BE. Tonotopic organization of the anteroventral cochlear nucleus of the cat. Hear Res 1981;4:215–241. [PubMed: 7263511]

Brown M, Shepherd RK, Webster WR, Martin RL, Clark GM. Cochleotopic selectivity of a multichannel scala tympani electrode array using the 2-deoxyglucose technique. Hear Res 1992;59:224–240. [PubMed: 1618713]

Busby PA, Tong YC, Clark GM. Electrode position, repetition rate, and speech perception by early- and late-deafened cochlear implant patients. J Acoust Soc Am 1993;93:1058–1067. [PubMed: 8445117]

Cant NB, Morest DK. The bushy cells in the anteroventral cochlear nucleus of the cat. A study with the electron microscope. Neurosci 1979;4:1925–1945.

Coco A, Epp SB, Fallon JB, Xu J, Millard RE, Shepherd RK. Does cochlear implantation and electrical stimulation affect residual hair cells and spiral ganglion neurons? Hear Res 2007;225:60–70. [PubMed: 17258411]

Fallon JB, Irvine DR, Shepherd RK. Cochlear implant use following neonatal deafness influences the cochleotopic organization of the primary auditory cortex in cats. J Comp Neurol 2009;512:101–114. [PubMed: 18972570]

Firszt JB, Chambers RD, Kraus N. Neurophysiology of cochlear implant users II: comparison among speech perception, dynamic range, and physiological measures. Ear Hear 2002;23:516–531. [PubMed: 12476089]

Franks KM, Bartol TM Jr, Sejnowski TJ. A Monte Carlo model reveals independent signaling at central glutamatergic synapses. Biophys J 2002;83:2333–2348. [PubMed: 12414671]

Gantz B, Tyler R, Woodworth G, Tye-Murray N, Fryauf-Bertschy H. Results of multichannel cochlear implants in congenital and acquired prelingual deafness in children: Five year follow up. Am J Otol 1994;15:1–8. [PubMed: 8572105]

Gentschev T, Sotelo C. Degenerative patterns in the ventral cochlear nucleus of the rat after primary deafferentation. An ultra-structural study. Brain Res 1973;62:37–60. [PubMed: 4765119]

Guillery RW. On counting and counting errors. J Comp Neurol 2002;447:1–7. [PubMed: 11967890]

Hardie NA, Martsi-McClintock A, Aitkin LM, Shepherd RK. Neonatal sensorineural hearing loss affects synaptic density in the auditory midbrain. NeuroReport 1998;9:2019–2022. [PubMed: 9674586]

Hardie NA, Shepherd RK. Sensorineural hearing loss during development: morphological and physiological response of the cochlea and auditory brainstem. Hear Res 1999;128:147–165. [PubMed: 10082295]

Hartshorn DO, Miller JM, Altschuler RA. Protective effect of electrical stimulation in the deafened guinea pig cochlea. Archives of Otolaryngology - Head and Neck Surgery 1991;104:311–319.

Hawkins JE Jr. Comparative otopathology: aging, noise, and ototoxic drugs. Adv Otorhinolaryngol 1973;20:125–141. [PubMed: 4710505]

Hultcrantz M, Snyder R, Rebscher S, Leake P. Effects of neonatal deafening and chronic intracochlear electrical stimulation on the cochlear nucleus in cats. Hear Res 1991;54:272–280. [PubMed: 1938629]

Keithley EM, Feldman ML. The spiral ganglion and hair cells of Bronx waltzer mice. Hear Res 1983;12:381–391. [PubMed: 6668259]

Kiang, NY-S.; Watanabe, T.; Thomas, EC.; Clark, LF. Discharge Patterns of Single Fibers in the Cat's Auditory Nerve. Cambridge, MA: MIT Press; 1965.

Klinke R, Kral A, Heid S, Tillein J, Hartmann R. Recruitment of the auditory cortex in congenitally deaf cats by long-term cochlear electrostimulation. Science 1999;285:1729–1733. [PubMed: 10481008]

Kotak VC, Sanes DH. Deafferentation weakens excitatory synapses in the developing central auditory system. Eur J Neurosci 1997;9:2340–2347. [PubMed: 9464928]

Kral A, Hartmann R, Tillein J, Heid S, Klinke R. Congenital auditory deprivation reduces synaptic activity within the auditory cortex in a layer-specific manner. Cereb Cortex 2000;10:714–726. [PubMed: 10906318]

Kral A, Tillein J, Heid S, Klinke R, Hartmann R. Cochlear implants: cortical plasticity in congenital deprivation. Prog Brain Res 2006;157:283–313. [PubMed: 17167917]

Kretzmer EA, Meltzer NE, Haenggeli CA, Ryugo DK. An animal model for cochlear implants. Arch Otolaryngol Head Neck Surg 2004;130:499–508. [PubMed: 15148168]

Laback B, Pok SM, Baumgartner WD, Deutsch WA, Schmid K. Sensitivity to interaural level and envelope time differences of two bilateral cochlear implant listeners using clinical sound processors. Ear Hear 2004;25:488–500. [PubMed: 15599195]

Larsen SA, Kirchoff TM. Anatomical evidence of plasticity in the cochlear nuclei of deaf white cats. Exp Neurol 1992;115:151–157. [PubMed: 1728561]

Leake PA, Hradek GT. Cochlear pathology of long term neomycin induced deafness in cats. Hear Res 1988;33:11–34. [PubMed: 3372368]

Leake PA, Hradek GT, Rebscher SJ, Snyder RL. Chronic intracochlear electrical stimulation induces selective survival of spiral ganglion neurons in neonatally deafened cats. Hear Res 1991;54(2):251–271. [PubMed: 1938628]

Leake PA, Hradek GT, Snyder RL. Chronic electrical stimulation by a cochlear implant promotes survival of spiral ganglion neurons after neonatal deafness. J Comp Neurol 1999;412:543–562. [PubMed: 10464355]

Leake PA, Stakhovskaya O, Hradek GT, Hetherington AM. Factors influencing neurotrophic effects of electrical stimulation in the deafened developing auditory system. Hear Res 2008;242:86–99. [PubMed: 18573324]

Lee DJ, Cahill HB, Ryugo DK. Effects of congenital deafness in the cochlear nuclei of Shaker-2 mice: an ultrastructural analysis of synapse morphology in the endbulbs of Held. J Neurocytol 2003;32:229–243. [PubMed: 14724386]

Lenn NJ, Reese TS. The fine structure of nerve endings in the nucleus of the trapezoid body and the ventral cochlear nucleus. Am J Anat 1966;118:375–390. [PubMed: 5917192]

Liberman MC. Auditory-nerve response from cats raised in a low-noise chamber. J Acoust Soc Am 1978;63:442–455. [PubMed: 670542]

Lissin DV, Gomperts SN, Carroll RC, Christine CW, Kalman D, Kitamura M, Hardy S, Nicoll RA, Malenka RC, von Zastrow M. Activity differentially regulates the surface expression of synaptic AMPA and NMDA glutamate receptors. Proc Natl Acad Sci USA 1998;95:7097–7102. [PubMed: 9618545]

Lustig LR, Leake PA, Snyder RL, Rebscher SJ. Changes in the cat cochlear nucleus following neonatal deafening and chronic intracochlear electrical stimulation. Hear Res 1994;74:29–37. [PubMed: 8040097]

Mair IW. Hereditary deafness in the white cat. Acta Otolaryngol 1973;314:1–48.

Matsuzaki M, Ellis-Davies GC, Nemoto T, Miyashita Y, Iino M, Kasai H. Dendritic spine geometry is critical for AMPA receptor expression in hippocampal CA1 pyramidal neurons. Nat Neurosci 2001;4:1086–1092. [PubMed: 11687814]

Mitchell A, Miller JM, Finger PA, Heller JW, Raphael Y, Altschuler RA. Effects of chronic high-rate electrical stimulation on the cochlea and eighth nerve in the deafened guinea pig. Hear Res 1997;105 (1–2):30–43. [PubMed: 9083802]

Moller AR. Unit responses in the rat cochlear nucleus to repetitive, transient sounds. Acta Physiol Scand 1969;75:542–551. [PubMed: 5358874]

Moore DR, Kowalchuk NE. Auditory brainstem of the ferret: Effects of unilateral cochlear lesions on cochlear nucleus volume and projections to the inferior colliculus. J Comp Neurol 1988;272:503–515. [PubMed: 2843582]

Moore JK, Niparko JK, Miller M, Linthicum F. Effect of profound deafness on a central auditory nucleus. Amer J Otol 1994;15:588–595. [PubMed: 8572057]

Niparko, JK.; Kirk, KI.; Mellon, NK.; Robbins, AM.; Tucci, DL.; Wilson, BS., editors. Cochlear Implants: Principles and Practices. Philadelphia: Lippincott Williams & Wilkins; 2000.

Noble W, Gatehouse S. Interaural asymmetry of hearing loss, Speech, Spatial and Qualities of Hearing Scale (SSQ) disabilities, and handicap. Int J Audiol 2004;43:100–114. [PubMed: 15035562]

O'Brien RJ, Xu D, Petralia RS, Steward O, Huganir RL, Worley P. Synaptic clustering of AMPA receptors by the extracellular immediate-early gene product narp. Neuron 1999;23:309–323. [PubMed: 10399937]

O'Neil JN, Limb CJ, Kretzmer EA, Baker CA, Ryugo DK. Bilateral Effects of Unilateral Cochlear Implantation in Congenitally Deaf Cats: A Critical Period for Synaptic Plasticity. Abst Assn Res Otolaryngol 2009;32:32.

Oleskevich S, Walmsley B. Synaptic transmission in the auditory brainstem of normal and congenitally deaf mice. J Physiol 2002;540:447–455. [PubMed: 11956335]

Powell TPS, Erulkar SD. Transneuronal cell degeneration in the auditory relay nuclei of the cat. J Anat 1962;96:219–268.

Quittner AL, Steck JT. Predictors of cochlear implant use in children. Am J Otol (Suppl) 1991;12:89–94.

Rubel, EW.; Parks, TN. Organization and development of the avian brain-stem auditory system. In: Edelman, GM.; Gall, WE.; Cowan, WM., editors. Auditory Function -Neurobiological Bases of Hearing. New York, Toronto, Singapore: John Wiley and Sons; 1988. p. 3-92.

Ryugo DK, Kretzmer EA, Niparko JK. Restoration of auditory nerve synapses in cats by cochlear implants. Science 2005;310:1490–1492. [PubMed: 16322457]

Ryugo DK, Montey KL, Wright AL, Bennett ML, Pongstaporn T. Postnatal development of a large auditory nerve terminal: the endbulb of Held in cats. Hear Res 2006;216–217:100–115.

Ryugo DK, Pongstaporn T, Huchton DM, Niparko JK. Ultrastructural analysis of primary endings in deaf white cats: Morphologic alterations in endbulbs of Held. J Comp Neurol 1997;385:230–244. [PubMed: 9268125]

Ryugo DK, Rosenbaum BT, Kim PJ, Niparko JK, Saada AA. Single unit recordings in the auditory nerve of congenitally deaf white cats: morphological correlates in the cochlea and cochlear nucleus. J Comp Neurol 1998;397:532–548. [PubMed: 9699914]

Ryugo DK, Wu MM, Pongstaporn T. Activity-related features of synapse morphology: A study of endbulbs of Held. J Comp Neurol 1996;365:141–158. [PubMed: 8821447]

Saada AA, Niparko JK, Ryugo DK. Morphological changes in the cochlear nucleus of congenitally deaf white cats. Brain Res 1996;736:315–328. [PubMed: 8930338]

Schwartz IR, Higa JF. Correlated studies of the ear and brainstem in the deaf white cat: Changes in the spiral ganglion and the medial superior olivary nucleus. Acta Otolaryngol 1982;93:9–18. [PubMed: 7064701]

Shepherd RK, Coco A, Epp SB, Crook JM. Chronic depolarization enhances the trophic effects of brain-derived neurotrophic factor in rescuing auditory neurons following a sensorineural hearing loss. J Comp Neurol 2005;486(2):145–158. [PubMed: 15844207]

Shepherd RK, Hardie NA. Deafness-induced changes in the auditory pathway: implications for cochlear implants. Audiol Neurootol 2001;6:305–318. [PubMed: 11847461]

Shepherd RK, Javel E. Electrical stimulation of the auditory nerve. I. Correlation of physiological responses with cochlear status. Hear Res 1997;108:112–144. [PubMed: 9213127]

Shepherd RK, Martin RL. Onset of ototoxicity in the cat is related to onset of auditory function. Hear Res 1995;92:131–142. [PubMed: 8647736]

Shepherd RK, Matsushima J, Martin RL, Clark GM. Cochlear pathology following chronic electrical stimulation of the auditory nerve: II Deafened kittens. Hear Res 1994;81:150–166. [PubMed: 7737922]

Shepherd, RK.; Meltzer, NE.; Fallon, JB.; Ryugo, DK. Consequences of deafness and electrical stimulation on the peripheral and central auditory system. In: Waltzman, SB.; Roland, TJ., editors. Cochlear Implants. 2. New York: Thieme Medical Publishers, Inc; 2006. p. 25-39.

Shepherd RK, Roberts LA, Paolini AG. Long-term sensorineural hearing loss induces functional changes in the rat auditory nerve. Eur J Neurosci 2004;20:3131–3140. [PubMed: 15579167]

Sly DJ, Heffer LF, White MW, Shepherd RK, Birch MG, Minter RL, Nelson NE, Wise AK, O'Leary SJ. Deafness alters auditory nerve fibre responses to cochlear implant stimulation. Eur J Neurosci 2007;26:510–522. [PubMed: 17650121]

Thai-Van H, Gallego S, Truy E, Veuillet E, Collet L. Electrophysiological findings in two bilateral cochlear implant cases: does the duration of deafness affect electrically evoked auditory brain stem responses? Ann Otol Rhinol Laryngol 2002;111:1008–1014. [PubMed: 12450176]

Trune DR. Influence of neonatal cochlear removal on the development of mouse cochlear nucleus: I. Number, size, and density of its neurons. J Comp Neurol 1982;209:409–424. [PubMed: 7130465]

Turrigiano GG, Leslie KR, Desai NS, Rutherford LC, Nelson SB. Activity-dependent scaling of quantal amplitude in neocortical neurons. Nature 1998;391:892–896. [PubMed: 9495341]

van Hoesel RJ, Tyler RS. Speech perception, localization, and lateralization with bilateral cochlear implants. J Acoust Soc Am 2003;113:1617–1630. [PubMed: 12656396]

Waltzman SB, Cohen NL, Shapiro WH. Effects of chronic electrical stimulation on patients using a cochlear prosthesis. Otolaryngol Head Neck Surg 1991;105:797–801. [PubMed: 1787969]

Webster DB. A critical period during postnatal auditory development of mice. Int J Pediatr Otorhinolaryngol 1983a;6:107–118. [PubMed: 6662618]

Webster DB. Late onset of auditory deprivation does not affect brainstem auditory neuron soma size. Hear Res 1983b;12:145–147. [PubMed: 6662826]

Webster M, Webster DB. Spiral ganglion neuron loss following organ of Corti loss: a quantitative study. Brain Res 1981;212:17–30. [PubMed: 7225854]

West CD, Harrison JM. Transneuronal cell atrophy in the deaf white cat. J Comp Neurol 1973;151:377–398. [PubMed: 4754840]

Wierenga CJ, Ibata K, Turrigiano GG. Postsynaptic expression of homeostatic plasticity at neocortical synapses. J Neurosci 2005;25:2895–2905. [PubMed: 15772349]

Yost WA. Discriminations of interaural phase differences. J Acoust Soc Am 1974;55:1299–1303. [PubMed: 4846726]

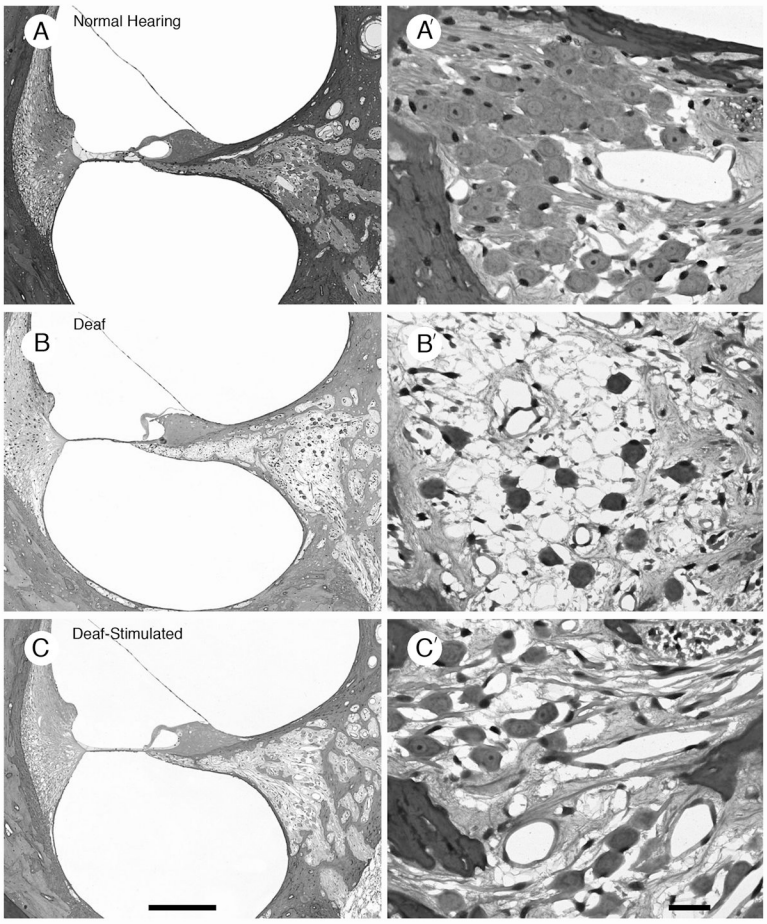

Figure 1.
Photomicrographs of histological sections of a representative cochlea from each cohort of cats. Low magnification micrographs taken through the basal turn (left column) and high magnification micrographs taken through Rosenthal's canal (right column) of normal, deaf, and deaf-stimulated animals, respectively. In normal hearing animals, organ of Corti is intact (A) and there is a full complement of spiral ganglion cells (A′). Hair cells are completely absent in the cochleae of deafened animals (B and C). Deaf (B′) and deaf-stimulated (C′) animals exhibit a striking loss of ganglion cells. Scale bar equals 250 μm for left column of panels and 25 μm for right column of panels.

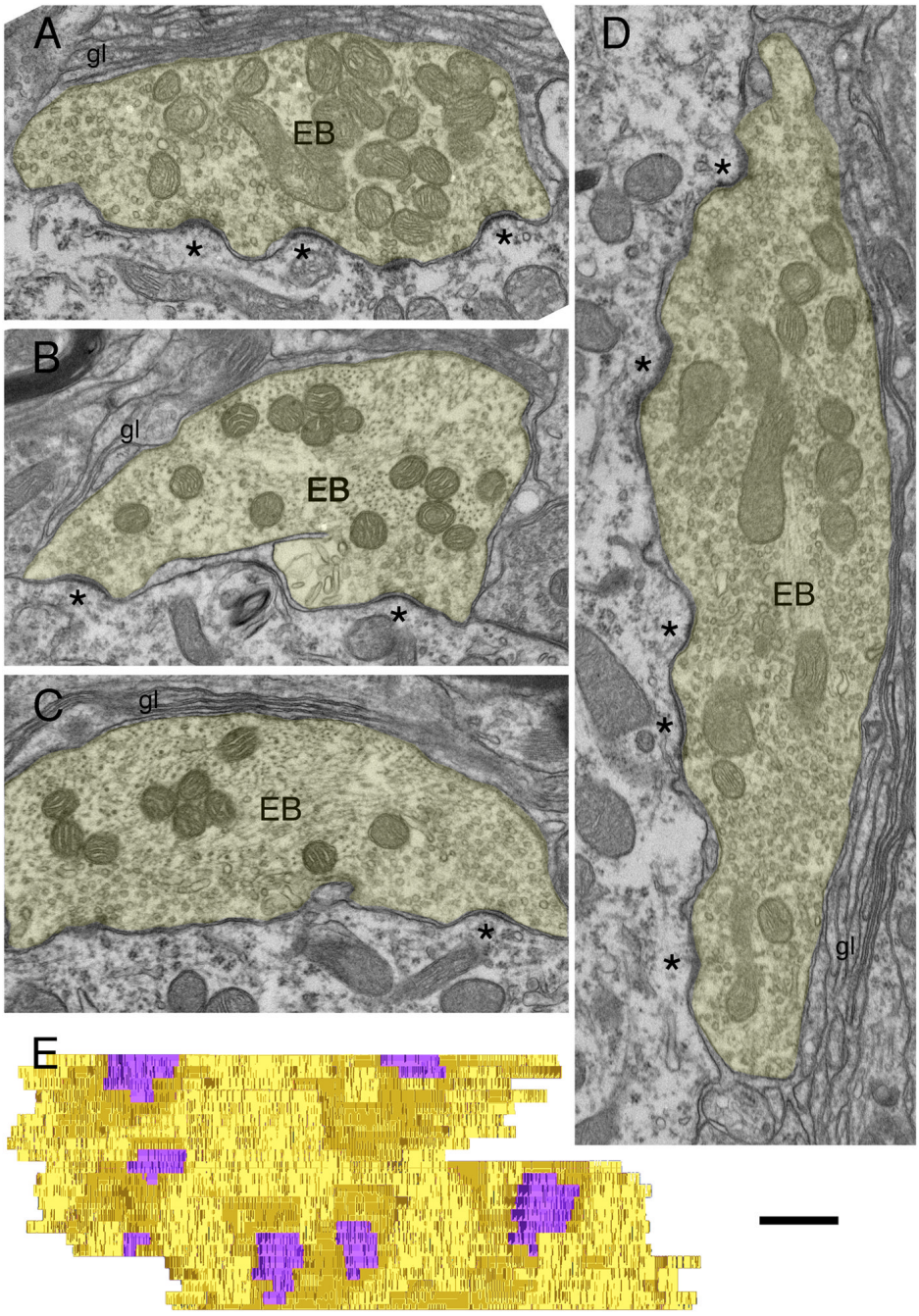

Figure 2.
Representative electron micrographs of endbulbs of Held (EB) of normal hearing cats (A–D). Note that the endbulbs have pale cytoplasm, contain round SVs (50–55 nm in diameter), and form asymmetric PSDs (*) on dome-shaped protrusions from the cell body of spherical bushy cells. Glial lamellae (gl) enclose the endings. The form of these synapses is characteristic of endbulbs from normal hearing cats. (E) *En face* view of reconstructed PSDs (purple) from consecutive serial sections. Note that the reconstructions reveal the PSDs to be punctate and relatively uniform in size. Scale bar equals 0.5 μm.

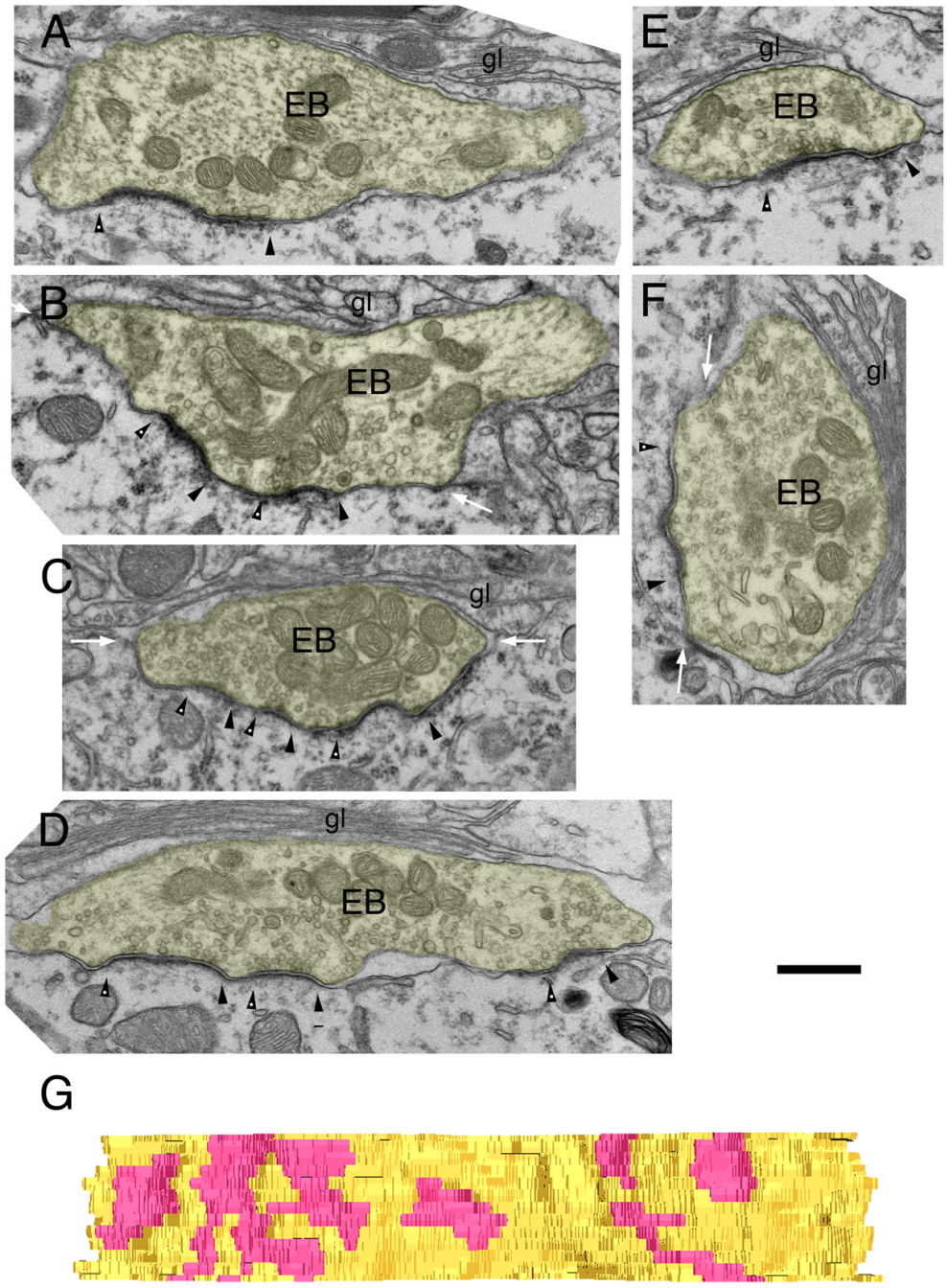

Figure 3.

Representative electron micrographs of endbulbs of Held (EB) of neonatally deafened cats. These animals had been ototoxically deafened for periods of 4.6–9.5 months. (A–F) The endings contain pale cytoplasm and are enveloped by glial lamellae (gl) but exhibit a loss of round SVs and a hypertrophy of the PSD. Each PSD is indicated by pairs of flanking arrowheads (left arrowhead of each pair has white dot). The PSDs are larger and lose their distinctive domed shape. Many PSDs tend to be flatter or wavy. These synapses are distinctly different in form from those of hearing cats. The white arrows (B, C, and F) indicate how the ending has indented the SBC surface. (G) The reconstructed PSDs (pink) demonstrate their larger size. Note also that there are normal sized PSDs in this (and all other) endings. Scale bar equals 0.5 μm.

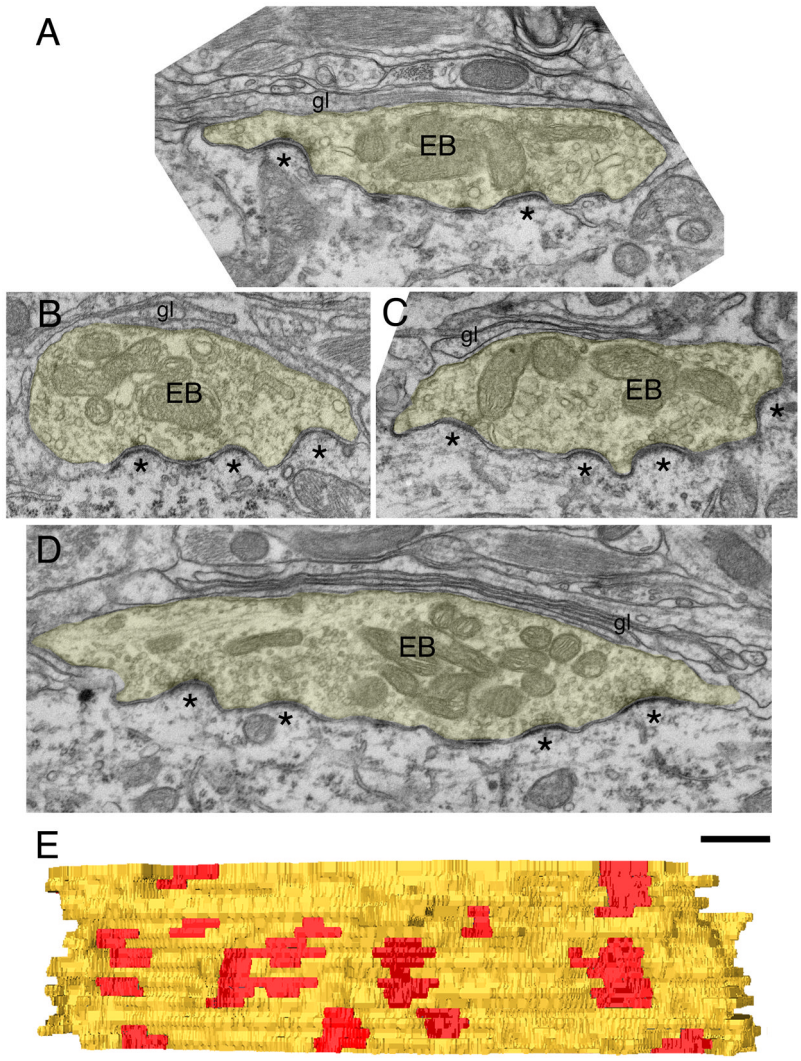

Figure 4.

Representative electron micrographs of endbulbs of Held (EB) from neonatally deafened cats whose auditory nerves were chronically stimulated via a cochlear implant. (A–D) These endings contain pale cytoplasm, are enveloped by glial lamellae (gl), and exhibit small but distinct accumulations of SV across from the PSDs (*). These endbulbs are ipsilateral to the cochlear implant and exhibit features of normal synapses. That is, PSDs reside on the dome-shaped swellings of the spherical bushy cell soma. (E) The reconstructed PSDs (red) are roughly the same size as PSDs in hearing cats. The more normal appearance of these synapses suggests that the restoration of spike activity in the auditory nerve restores synaptic morphology. Scale bar equals 0.5 μm.

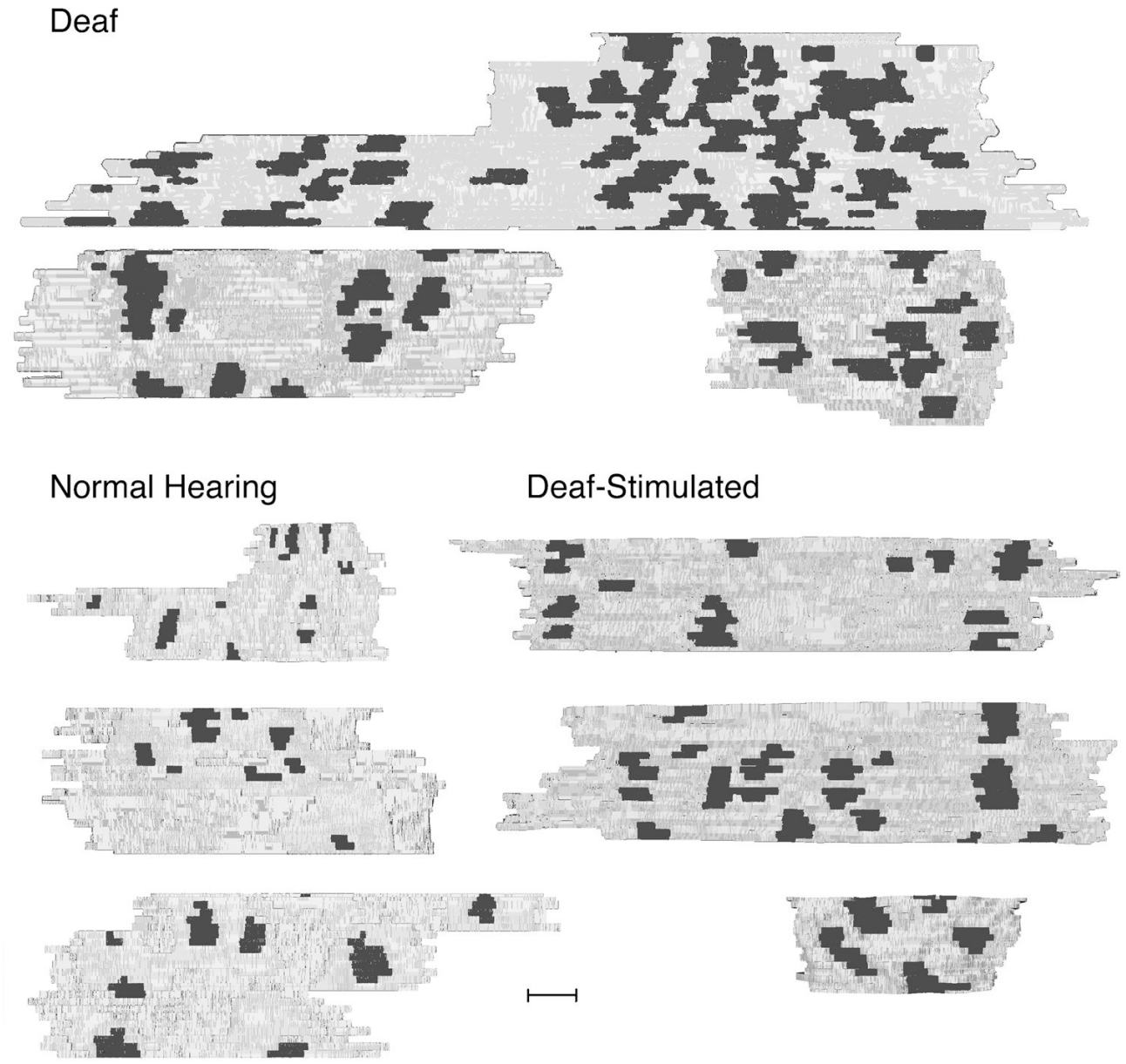

Figure 5.

En face view of PSD reconstructions derived from serial section electron micrographs of endbulbs. Unbroken strings of sections through individual endbulbs were photographed, digitized, aligned, stacked, and rotated using *Adobe Photoshop* and *Amira* software. The views represent the surface of the spherical bushy cell (grayish) lying beneath the endbulb. Note that the PSDs (dark) are hypertrophied in the endbulbs from deaf cats, whereas those from normal hearing and stimulated cats have PSDs of similar size and distribution. Scale bar equals 0.5 μm.

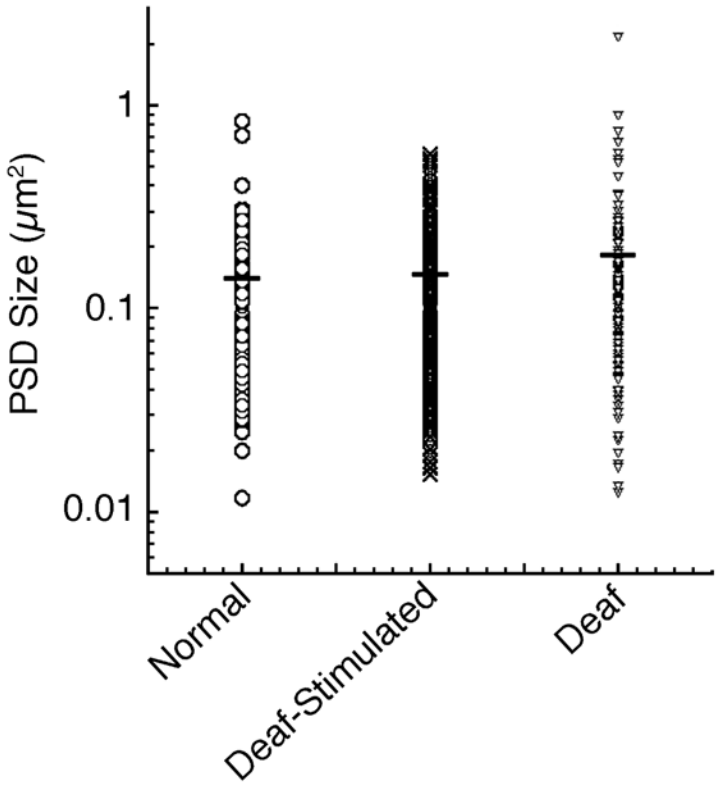

Figure 6.
Data plot for all PSD measurements. It is noteworthy that many PSDs are roughly normal in size regardless of the status of the cat.

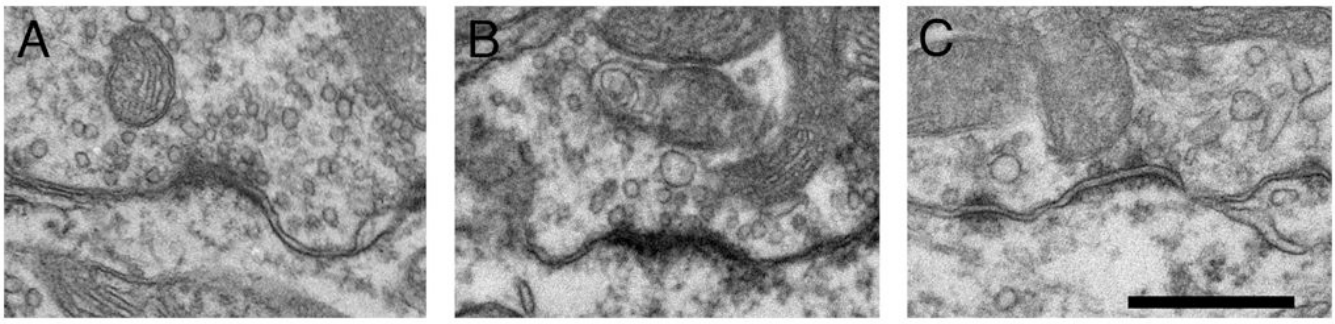

Figure 7.
Electron micrographs of synapses representative of the different cohorts: (A) normal hearing cart; (B) ototoxically deafened cat; (C) ototoxically deafened cat with electrical stimulation. Synaptic vesicle size and shape does not change across cohorts, but synaptic density around the PSD is significantly reduced in both cohorts of deafened cats. Scale bar equals 0.5 μm.

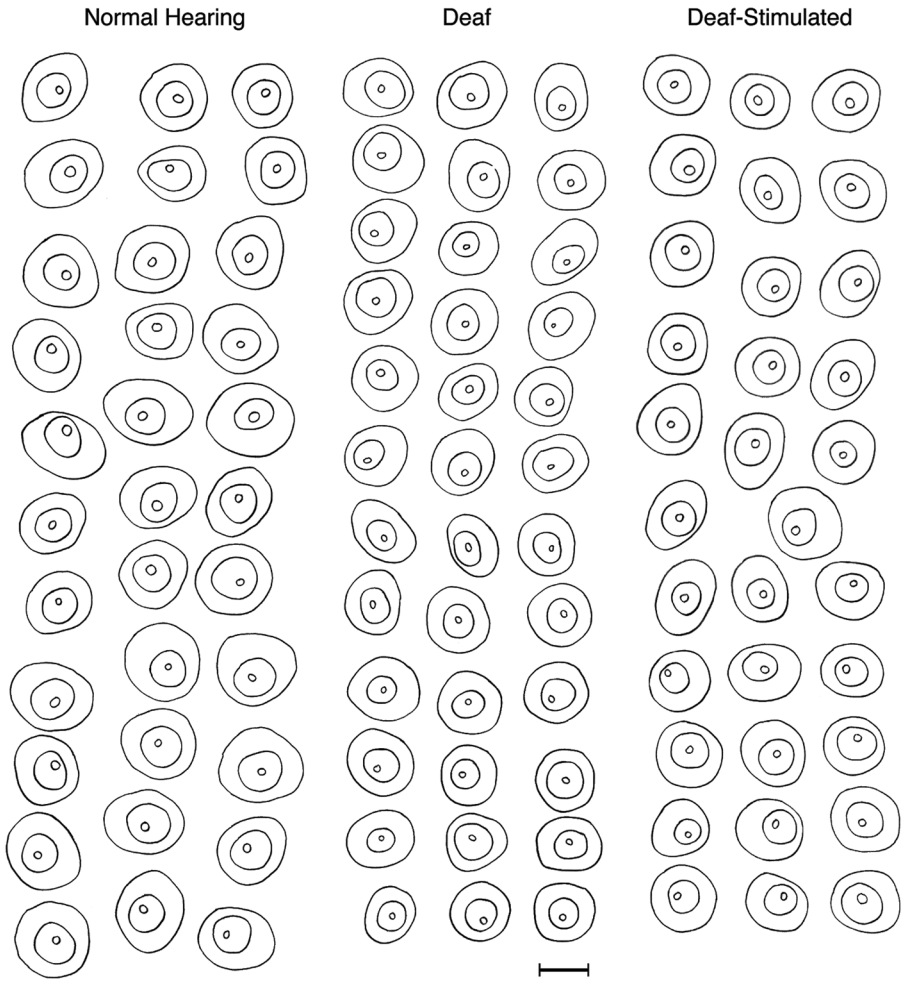

Figure 8.

Drawing tube reconstructions of spherical bushy cells from the anteroventral cochlear nucleus of normal hearing, deaf, and deaf-stimulated cats. These cells were selected from the high frequency region (>10 kHz) of the AVCN. Bushy cells from hearing cats are roughly 20% larger than those of ototoxically deafened cats and approximately 25% larger than those of deaf-stimulated cats. These data suggest that stimulation by itself does not induce cell bodies to grow to their normal size. Scale bar equals 20 μm.

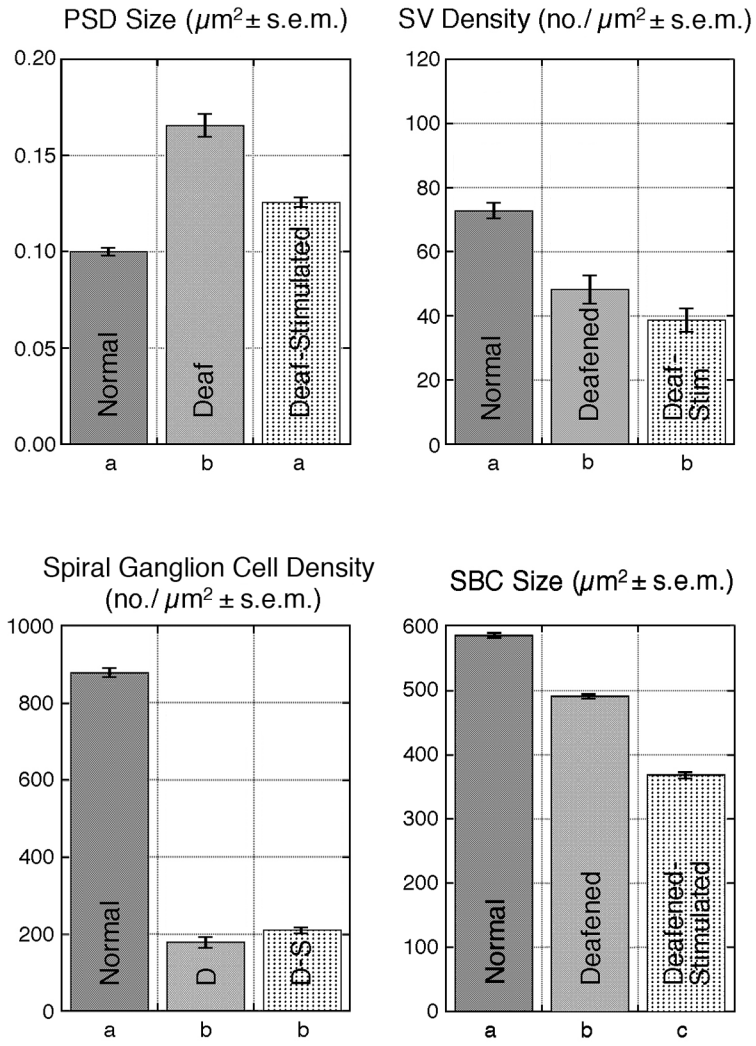

Figure 9.

Bar graphs comparing PSD size, SV density, spiral ganglion cell density, and spherical bushy cell (SBC) somatic size across the cohorts of normal hearing cats, ototoxically deafened cats, and deafened and stimulated cats. The letters, *a*, *b*, *and c*, below the graphs indicate statistical difference when the letters are different ($p<0.05$, Kruskal-Wallis test). The plots illustrate the hypertrophy of PSDs in deaf animals and the return to normal size of the PSDs in deaf-stimulated cats. There is also loss of presynaptic SVs, loss of spiral ganglion cells, and somatic shrinkage of the SBCs in deafened cats; these changes are not ameliorated by stimulation via a cochlear implant.

Table 1

Animal I.D.	Status	Sex	Hearing Status (Duration of Ototoxic Treatment in days)	Electrode Pairs	Age at Sacrifice (months)	Stim Duration (Weeks)	No. EBs	PSD size (sq. nm ± S.D.)	SV density (SVs/sq. µm ±S.D.)	SGN density (cells/sq.mm ± S.D.)
05_943	Normal Hearing	F	Normal hearing		11.0		10	0.109 ± 0.05 n = 54	75.62 ± 15.1	797.55 ± 224.5
05_947	Normal Hearing	F	Normal hearing		8.0		5	0.065 ± 0.03 n = 27	69.21 ± 16.7	954.40 ± 264.1
05_949	Normal Hearing	F	Normal hearing		13.0		5	0.118 ± 0.08 n = 26	77.18 ± 22.0	916.96 ± 208.2
04_929	Deafened stimulated	M	profoundly deaf (17)	1/2 and 6/7	4.6	10.7	10	0.156 ± 0.08 n = 39	28.61 ± 11.4	329.50 ± 111.4
04_934	Deafened stimulated	M	profoundly deaf (21)	cg 1, cg 2	11.7	40.4	3	0.124 ± 0.11 n = 28	42.99 ± 10.9	259.14 ±98.1
04_935	Deafened stimulated	M	profoundly deaf (17)	cg 1, cg 3	9.6	29.9	10	0.115 ± 0.12 n = 35	43.93 ± 22.5	255.51 ± 70.1
04_937	Deafened stimulated	F	profoundly deaf (21)	cg 1, cg 2	14.0	46.4	3	0.145 ± 0.15 n = 12	26.17 ± 13.5	65.95 ± 32.5
04_938	Deafened stimulated	M	profoundly deaf (17)	1 v 2,6,7,8	7.4	21.6	8	0.152 ± 0.02 n = 53	46.77 ± 16.1	154.60 ± 99.8
03_924	Deafened control	F	profoundly deaf (24)		10.3		8	0.170 ± 0.16 n = 45	15.39 ± 11.6	127.88 ± 63.2
03_925	Deafened control	M	profoundly deaf (21)		10.3		12	0.117 ± 0.07 n = 52	69.64 ± 14.0	202.19 ± 116.6
04_932	Deafened control	F	profoundly deaf (21)		7.9		7	0.188 ± 0.27 n = 87	46.49 ± 12.7	200.96 ± 101.7